# A CO-PRODUCING DIRECT CARBON FUEL CELL WITH MOLTEN CARBONATE ELECTROLYTE

A.elleuch, A. boussetta and K. halouani*
*IESG – METS, IPEIS, University of Sfax, route menzel chaker km 0.5, BP: 1172, 3018*
kamel.halouani@ipeis.rnu.tn, amal-elleuch@hotmail.com, ahlemkacem2004@yahoo.fr

## ABSTRACT
The direct carbon fuel cell (DCFC) is a high temperature fuel cell that directly uses solid carbon particles as anode and fuel. It has great thermodynamic advantages over other high temperature fuel cells such as MCFC and SOFC. It can have 100 % fuel utilization, a higher achievable efficiency of about 80% and less emission than conventional coal-burning power plants [1]. In this work, a fundamental study of the electrochemical phenomena within the DCFC is developed with a supposed packed bed anode structure. Polarizations within the DCFC are examined supposing graphite as anode and molten carbonate as electrolyte. The obtained results lead to understand the effect of CO produced in the anode side at high temperature (1000 K to 1100 K) on the performance of the DCFC.

## NOMENCLATURE

| | | |
|---|---|---|
| $b_i$ | Diameter of the contact area between two carbon particles | (m) |
| $C_i^B$ | Bulk molar concentration of species i | (mol.m$^{-3}$) |
| $C_i^S$ | Surface molar concentration of species i | (mol.m$^{-3}$) |
| $D_c$ | Carbon particle diameter | (m) |
| $D_i$ | Diffusion coefficient of species i | (m$^2$.s$^{-1}$) |
| $E$ | Ideal potential | (V) |
| $F$ | Faraday constant | (C.mol$^{-1}$) |
| $i$ | Current density | (A.m$^{-2}$) |
| $i_{0e}$ | Exchange current density of the electrode e (anode, cathode) | (A.m$^{-2}$) |
| $i_{li}$ | Limit current density of species i | (A.m$^{-2}$) |
| $n_e$ | Electron number | |
| $P_i$ | Partial pressure of species i | (atm) |
| $R_{c,i}$ | Resistance in the anodic electrode | (S$^{-1}$) |
| $R_{ce}$ | Resistance in the cathode and the electrolyte | (m$^2$S$^{-1}$) |
| $R_{ohmic}$ | Ohmic resistance | (m$^2$S$^{-1}$) |
| $R_{s,i}$ | Resistance in the electrolyte | (S$^{-1}$) |
| $T$ | Operating temperature | (K°) |
| $V$ | Cell voltage | (V) |
| $y$ | Length of the packed bed anode | |
| $z$ | Width of the packed bed anode | |
| $\varepsilon$ | Porosity of the packed bed anode | (S.m$^{-1}$) |
| $\eta_{ohmic}$ | Ohmic overpotential | (V) |
| $\eta_{act,e}$ | Activation overpotential of the electrode e (anode, cathode) | (V) |
| $\eta_{conc,e}$ | concentration overpotential of the electrode e (anode, cathode) | (V) |
| $v_i$ | Stochiometric coefficient of the species i | |
| $v_e$ | Stochiometric coefficient of the electron | |
| $n_e$ | Electron number | |
| $\delta_e$ | Thickness of porous electrode side e (anode, cathode) and the electrolyte | (m) |
| $\sigma_e$ | Conductivity coefficient electrode side e (anode, cathode) and the electrolyte | (S. m$^{-1}$) |

## 1. INTRODUCTION

Direct Carbon Fuel Cells offer specific thermodynamic advantages compared to other fuel cell types. DCFCs electrochemically convert solid carbon fuel into $CO_2$ and/or carbon monoxide (CO). Because the entropy change in the overall cell reaction is around zero (for $CO_2$ as reaction product) or even positive (for CO as product), the theoretical reversible electric efficiency (commonly defined as $\Delta G/\Delta H$ of the overall cell reaction) of a DCFC can be around 100 % [2]. The development of DCFCs has been limited by low anode reaction rates, accumulation of impurities in the electrolyte and logistics of refueling the cell. These problems are being addressed by recent developments in the production of clean and highly reactive carbon materials (e.g. from natural gas), low-cost techniques for separation of ash from coal, the possibility of pneumatic distribution of solid particulate fuel to the cells or the use of a slurry of carbon particles in a molten carbonate and the availability of technology developed for the MCFC developments (electrodes and electrolytes) [2].The objective of this research is to present a CO-producing DCFC system model with simulation outcomes in order to provide a theoretical basis for DCFC (system) performance by using the temperature as a parameter responsible of weather the CO or $CO_2$ production at the carbon electro-oxidation reaction.
In this paper, a DCFC electrochemical modeling is presented and the effect of maintaining the CO production on the DCFC performance is determined. The effects of temperature on the polarization of a CO-producing DCFC system or a $CO_2$-producing one are also examined.

## 2. THE $CO_2$ –PRODUCING DCFC SYSTEM MODELING

In this section, the $CO_2$-producing DCFC system is modeled in order to study the performance of the direct carbon fuel cell. The two electrodes reactions occurring within this type of DCFC based molten carbonate electrolyte are presented as follows [3, 4]:

Anode reaction: $C + 2\ CO_3^{2-} \rightarrow 3\ CO_2 + 4e^-$ (1)

Cathode reaction: $O_2 + 2\ CO_2 + 4e^- \rightarrow 2CO_3^{2-}$ (2)

The overall DCFC reaction is: $C + O_2 \rightarrow CO_2 \qquad E° = 1.02\ V$ (3)

As the DCFC system includes complex electrochemical phenomena, its performance is strongly affected by the corresponding losses called respectively activation polarization ($\eta_{act}$), ohmic polarization ($\eta_{ohmic}$) and concentration polarization ($\eta_{conc}$). The proposed model is based on direct oxidation of carbon to $CO_2$ at the anode side and uses Fick's model to evaluate the concentration polarization, the Buttler-Volmer equation to calculate the activation polarization when ohmic polarization is expressed by the well known Ohm's law.
These losses ($\eta_T$) make lower the cell voltage ($V$) compared to the ideal potential ($E$) as:

$$V = E - \eta_T \qquad \text{ou} \qquad \eta_T = \left|\eta_{act,c} + \eta_{conc,c}\right| - \left|\eta_{act,a} + \eta_{conc,a}\right| + \eta_{ohmic} \tag{4}$$

The ideal potential is given by the Nernst equation which is function of the partial pressure of gaseous species existing within the $CO_2$-producing DCFC system [5].

$$E = E_T^\circ + \frac{RT}{4F}\ln\left(\frac{P_{O_2}}{P_{CO_2}}\right) \tag{5}$$

Where $E_T^\circ = -\Delta G_T^\circ/(4F)$, $E_T^\circ$ and $\Delta G_T^\circ$ are respectively the ideal potential and the Gibbs free energy at standard pressure and temperature $T$.

### 2.1. Activation polarization

The Buttler -Volmer equation describes well the activation polarization as follows:

$$i_e = i_{0e}\exp\left(\frac{\alpha_e \eta_{act,e}(n_e F)}{RT}\right) - i_{0e}\exp\left(\frac{-(1-\alpha_e)\eta_{act,e}(n_e F)}{RT}\right) \tag{6}$$

The coefficient $\alpha_a$ is the anodic charge transfer coefficient which has a value of 0.25 [6]. Thereafter, the coefficient of charge transfer at the cathode side ($\alpha_c$) is about 0.75 [3].

### 2.2. Ohmic polarization

The ohmic polarization appears due to the resistance to ion flow in the electrolyte and electron flow through electrodes. It obeys to Ohm's law and is expressed by the equation:

$$\eta_{ohmic} = R_{ohmic} \times i \quad (7)$$

Where $i$ is the current flowing through the unit cell, and $R_{ohmic}$ is the total unit cell resistance, which includes electronic, ionic, and contact resistances [7].

In this part, we supposed new structure of the anode side to determine the ohmic losses. This new structure is composed from solid carbon fuel in the form of particles wetted with molten salt. Each particle is assumed to act as a rigid sphere and packed with a simple hexagonal pattern [8].

For the anode, the resistance in each slab contains two parts, i.e. the resistances in the electrolyte $R_{s,i}$ and in the electrode $R_{c,i}$ in the slab $i$, respectively. The $R_{s,i}$ is expressed as[8]:

$$R_{s,i} = D_c / \sigma_s yz\varepsilon^{1.5} \quad (8)$$

The conductivity of the electrolyte which is a 62/38 $Li_2CO_3/K_2CO_3$ is a function of temperature and obeys to Arrhenius' law [9]: $\sigma_s = \sigma_s^0 \exp(-E_a / RT)$ (9)

The current flow through the electrolyte phase and the electrode are expressed respectively by [8]:

$$i_{s,i} = i(1 - 2\Pi(N_s - 1)).y.z.\varepsilon^{1.5} \quad (10)$$

$$i_{c,i} = 2\Pi i\ (N_s - 1).S_i \quad (11)$$

The number of slab within the anode is a function of the carbon graphite diameter $D_c$ and anode thickness $\delta_a$ and is defined as: $N_s = \delta_a / D_c$ (12)

Moving to the $R_{c,i}$ which is defined as a function of the diameter of the contact area between two particles ($b_i$) [8].

$$R_{c,i} = 1 / \sigma_c b_i \quad (13)$$

The contact area $S_i$ is dependent on the forces $F$ acting on the particles and the mean yield pressure of the asperities ($P_m$) is presented as the following [8]:

$$S_i = F_i / P_m \quad (14)$$

The forces applied on the particles include gravitational force $F_{g,i}$ , buoyancy force $F_{f,i}$ and repulsive force $F_{r,i}$ [8]. However, the repulsive force on the top and the bottom of carbon particle is assumed to be equal. Consequently, the difference of gravitational force and buoyancy force is the force pressing the particles ($F_i$): $F_i = (N_s - 1)(F_{f,i} - F_{g,i})$ (15)

With: $F_{f,i} = 1.33\rho_s \Pi g D_c^2$ (16)

$$F_{g,i} = 1.33\rho_c \Pi g D_c^2 \quad (17)$$

After determining the two type of resistance occurring in the anodic part, we will move to express the resistances of the other parts (cathode and electrolyte) as follows [10]:

$$R_{ce} = (A / P_{O2}^{0.67}) \exp(B/T) + C_R + D\exp(f/T) \quad (18)$$

Where $P_{O2}$ is the partial pressure of oxygen at the cathode surface and $D$ is a kinetic parameter related to the electrolyte content of the matrix.

In fact, the total ohmic polarization will be expressed using this expression [8]:

$$\eta_{ohmic} = \sum_{i=1}^{N_s} i_{s,i} R_{s,i} + \sum_{I=1}^{N_s} i_{c,i} R_{c,i} + iR_{ce} \quad (19)$$

### 2.3. Concentration polarization

Several processes may contribute to concentration polarization: slow diffusion of the gas species ($CO_2$, $O_2$), solution /dissolution of reactants and products into and out of the electrolyte, or diffusion of reactants and products through the electrolyte to and from the electrochemical reaction site.
The concentration polarization within the $CO_2$- producing DCFC system is defined using the Fick's law [11] as the following:

$$\eta_{conc} = \frac{RT}{F}\left(\frac{1}{4}\ln\left(1-\frac{i}{i_{lO2}}\right)+\frac{1}{2}\ln\left(1-\frac{i}{i_{lCO2}}\right)-\frac{3}{4}\ln\left(1-\frac{i}{i_{lCO2}}\right)\right) \quad (20)$$

The term $i_{li}$ is the limiting current density given by:

$$i_{li} = nFD_i\left(\nu_e/\nu_i\right)\left(C_i^B/\delta\right) \quad (21)$$

The bulk concentration ($C_i^B$) is determined using Henry's law [12]: $C_i^B = K_i \times P_i$, where $K_i$ is the solubility for dissolved gases.

## 3. THE CO-PRODUCING DCFC SYSTEM MODELING

In the literature, the CO formation in the anode side is always neglected. But referring to the operating range of temperature (900 K to 1100 K), we can notice that the formation of CO must be considered. This could be explained by the fact that the CO concentration increases with rising cell temperature but the $CO_2$ concentration increases slightly from 600 to 700 °C and decreases sharply at 800 °C. This phenomenon may be caused by the following Boudouard reaction that can easily occur at temperatures above 750°C and it has as a role to consume the formed $CO_2$ and carbon in reaction (1) at higher temperature [13]: :

$$CO_2 + O_2 \rightarrow CO \quad (22)$$

In fact, the anode reaction moves from producing $CO_2$ and 4 electrons following reaction 1 to this anodic reaction [13]: $C + CO_3^{2-} \rightarrow CO + CO_2 + 2e^-$ (23)
Consequently, the overall reaction of the CO-producing DCFC system will be [2]:

$$C + ½\ O_2 \rightarrow CO \quad (24)$$

The CO- producing DCFC system based on the same activation and ohmic polarization formulation developed in the last section. The concentration polarization and the ideal potential of the CO-producing DCFC system are elaborated by considering the simultaneous formation of CO and $CO_2$ at the anode side illustrated in this global electrochemical reaction [14]:

$$\left\{n_C C + n_{CO_2)a} CO_2 + n_{CO} CO\right\} + \left\{n_{CO_2)c} CO_2 + n_{O_2} O_2\right\} \rightarrow n_{p\,CO_2}\ CO_2 + n_{p\,CO} CO \quad (25)$$

At the equilibrium, these molar numbers are related by the following relations:

$$n_{CO_2)c} + n_{CO_2)a} + n_C + n_{CO} = n_{PCO2} + n_{PCO} \quad (26)$$

$$2\,n_{CO_2)c} + 2n_{CO_2)a} + 2n_{O_2} + n_{CO} = 2n_{PCO2} + n_{PCO} \quad (27)$$

### 3.1. The ideal potential

The ideal potential for reaction is given by the Nernst equation [14]:

$$E_T = E_T^\circ + \frac{RT}{n_e F}\left(n_c \ln\left(\frac{P_C}{P_{anode}}\right) + n_{02}\ln\left(\frac{P_{O2}}{P_{cathode}}\right) + n_{CO2)c}\ln\left(\frac{P_{CO2)c}}{P_{cathode}}\right) + n_C \ln\left(\frac{P_{CO2)a}}{P_{anode}}\right)\right.$$
$$\left. - n_{GO2)c}\ln\left(\frac{P_{CO2)a}}{P_{anode}}\right) - 2n_{O2}\ln\left(\frac{P_{CO2)a}}{P_{anode}}\right) - 2n_C \ln\left(\frac{P_{CO}}{P_{anode}}\right) + 2n_{O2}\ln\left(\frac{P_{CO}}{P_{anode}}\right)\right) \quad (28)$$

Where $n_e$ is the total number of electrons transferred and is given by $n_e = 2\ n_C$

### 3.2. The concentration polarization

The Fick's law is employed to define the concentration polarization in the CO-producing DCFC system. In fact, the cathodic concentration loss will be presented as follows [14]:

$$\eta_{conc,c} = \frac{RT}{n_e F}\left(n_{O_2}\ln\left(\frac{C_{O_2}^S}{C_{O_2}^B}\right) + n_{O2}\ln\left(\frac{C_{CO_2}^S}{C_{CO_2}^B}\right)\right)$$

(29)

At the anode side, it is expressed as follows [14]:

$$\eta_{conc,a} = \frac{RT}{n_e F}\left(n_C \ln\left(\frac{C_C^S}{C_C^B}\right) + n_C \ln\left(\frac{C_{CO_2)a}^S}{C_{CO_2)a}^B}\right) - n_{CO_2)c} \ln\left(\frac{C_{CO_2)a}^S}{C_{CO_2)a}^B}\right) - 2\, n_{O_2} \ln\left(\frac{C_{CO_2)a}^S}{C_{CO_2)a}^B}\right)$$

$$- n_C \ln\left(\frac{C_{CO}^S}{C_{CO}^B}\right) + 2\, n_{O_2} \ln\left(\frac{C_{CO}^S}{C_{CO}^B}\right)) \quad (30)$$

A calculation code based on a mathematical formulation of the electrochemical phenomena discussed above is solved using MATLAB code in order to study the performance of the CO and $CO_2$ producing DCFC system and to detect the effect of operating conditions.

## 4. SIMULATION RESULTS

The evolution of polarization curve of a $CO_2$-producing DCFC system presented in figure 2 at a temperature of 1000 K is compared with those of Vutetakis and shows a good agreement with an average absolute deviation (*AAD*) of about 8 %. This can be explained by the hypothesis of homogeneous temperature within all DCFC's compartment used in our model.

Figure 2 shows the effect of the high concentration of CO within the DCFC at a temperature of 1000 K. The first effect is clear in the *OCP* which move from 1.02 when modelling a $CO_2$-producing DCFC system to 1.24 when modelling a CO-producing DCFC system. This could be evident due to the Boudouard equilibrium which shifts towards more CO and less $CO_2$ at this high operating temperature. The second oxidation reaction (23) that took place in the anode side will present an additional parallel reaction path. So, an increase in the resistance within the DCFC will automatically decrease the ohmic polarization. The high concentration of carbon monoxide affects the diffusion of the gases species produced in the anode side within the membrane so decreases the concentration polarisation within the CO-producing DCFC system compared to the $CO_2$-producing one. We can notice also, that the CO production contributes in ameliorating the DCFC performance. In fact the maximum power density moves from 270 W/m$^2$ with a $CO_2$-producing DCFC system to 333 W/m$^2$ with a CO-producing DCFC system.

Hence, Producing the carbon monoxide present an important precursor in enhancing DCFC performance firstly and in the chemical industry field, for instance in the production of syngas [15].

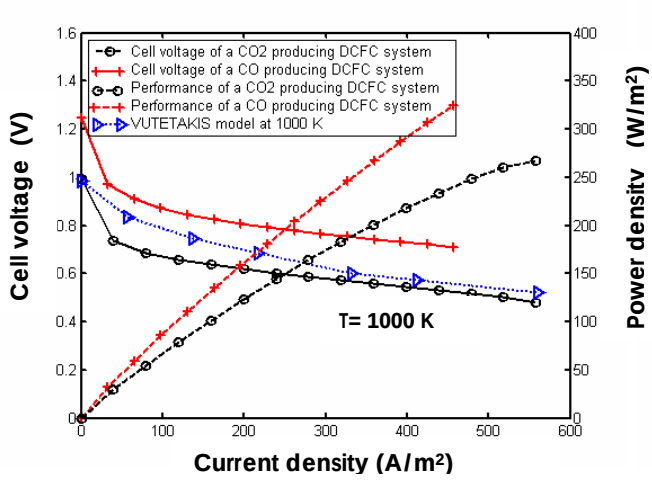


Figure 2. Polarisation curve of a CO and $CO_2$ producing DCFC system.

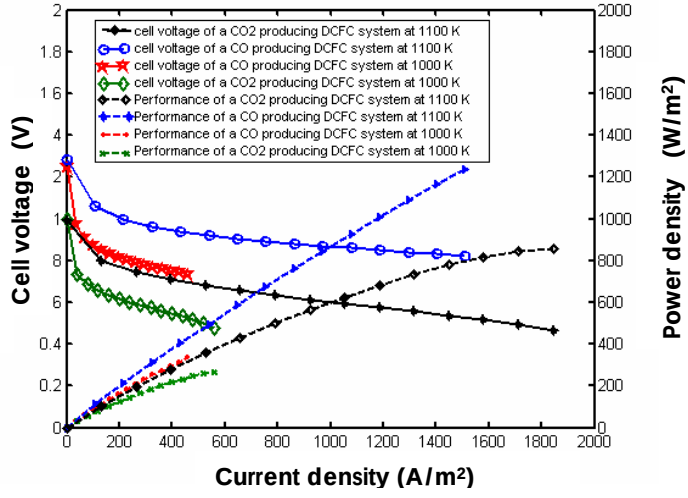


Figure 3. Temperature effect on the polarization curve of DCFC.

Figure 3 shows that raising in temperature plays a significant role in achieving a high performance within the DCFC system whatever we talk about a CO and a $CO_2$ producing one.

In fact, the maximum power density of a CO producing DCFC system move from 333 W/m$^2$ at 1000 K to 1219 W/m$^2$ at 1100 K and from 270 W/m$^2$ to 860 W/m$^2$ at a $CO_2$ producing DCFC system. This could be explained by the fact that at high temperature, the electrodes became more reactive and the anodic reaction kinetics was enhanced. So, the activation polarization decreases with rising temperature. We can also notice that, the conductivity of the DCFC materials is inversely proportional to temperature. So, the resistivity and consequently the ohmic losses increase with rising temperature.

## 4. CONCLUSION

An analytical investigation of the electrochemical mechanisms is developed to study the effect of CO production within the DCFC anode at high temperature. The rising in performance seems more reasonable since at high temperature the Boudouard equilibrium prefers CO over $CO_2$. So, the carbon electro-oxidation to carbon monoxide offers large thermodynamic advantages and a good amelioration in the performance.

## REFERENCES BIBLIOGRAPHIQUES

[1] D. Cao, Y. Sun, G. Wang, 2007, direct carbon fuel cell: fundamentals and recent developments, Journal of Power Sources, vol. 167, pp. 250-257.
[2] K.Hemmes, M. Houwing, N.Woudstra, Modelling of a direct carbon fuel cell system, the Third International Conference on fuel cell Science, Engineering and Technology, Ypsilanta, Michingan,2005.
[3] A.Kornhauser, Modelling and design for a direct carbon fuel cell with entrained fuel and oxidizer, 2005.
[4] K. Pointon, B. Lakeman , J. Irvine, J.Bradley, Sneh Jain, 2006, the development of a carbon- air semi fuel cell, Journal of Power Sources, vol. 162, pp. 750-756.
[5] G. A. Hackett, J. W. Zondlo a, R. Svensson, 2007, Evaluation of carbon materials for in a direct carbon fuel cell, vol. 168, pp. 111-118.
[6] R.F. Mann, J.C. Amphlett, B.A. Peppley, C.P. Thurgood, 2006, Application of Butler–Volmer equations in the modelling of activation polarization for PEM fuel cells, Journal of Power Sources, vol. 161, pp. 775–781.
[7] Th. Aloui ,K. Halouani, 2007 , Analytical modeling of polarizations in a solid oxide fuel using biomass syngas product as fuel, Applied Thermal Engineering, vol. 27, pp. 731-737.
[8] Q. Liu, Ye. Tian, Ch.Xia, Levi T. Thompson, Bin Liang, Y. Li, 2008, modelling and simulation of a single direct carbon fuel cell, Journal of Power Sources, vol. 185, pp. 1022-1029.
[9] T. Kojima, Y. Miyazaki, K. Nomura, K. Tanimoto, 2007, Electrical conductivity of molten $Li_2CO_3$- $X_2CO_3$ (X: Na,K, Rb, and Cs) and $Na_2CO_3$- $Z_2CO_3$ (Z: K, Rb, and Cs) Journal of Electrochemical Society, vol. 154 (12), pp. F222-F230.
[10] B.Bosio, P. Costamagna, F. Parodi, 1999 , Modeling and experimentation of molten carbonate fuel cell reactors in a scale-up process , Chemical engineering Science, vol. 54, pp. 2907-2916.
[11] B.Basio, E.Arato, P.Costa, 2003, concentration polarization in heterogeneous electrochemical reactions a consistent kinetic evaluation and its application to molten carbonate fuel cells, Journal of Power Sources, vol. 115, pp.189-193.
[12] G.Wilemski, 1983, simple porous electrode models carbonate fuel cells, Journal of Electrochemical Society, vol. 130, n°1, pp. 117-121.
[13] X, Li, Z. Zhu, J. Chen, R. De Marco, A. Dicks, J. Bradely, G. Lu, 2009, surface modification of carbon fuels for direct carbon fuel cell, Journal of Power Sources, vol. 186, pp. 1-9.
[14] H.Zhu, Robert J .Kee, 2003, a general mathematical model for analysing the performance of fuel-cell membrane-electrode assemblies, Journal of Power Sources, vol. 117, pp.61-74.
[15] W.H.A.Peelen, K.Hemmes, J.H.W.de Wit, 1998, carbon a major energy for the future? Direct carbon fuel cells and molten salt coal/biomass gasification, European research conference on molten salts, Poquerolles, France.